THE JOURNAL OF PHYSICAL CHEMISTRY B

ARTICLE

pubs.acs.org/JPCB

Density Functional Study of the Electric Double Layer Formed by a High Density Electrolyte

Douglas Henderson,*,† Stanisław Lamperski,‡ Zhehui Jin,§ and Jianzhong Wu§

†Department of Chemistry and Biochemistry, Brigham Young University, Provo Utah 84602-5700, United States

‡Department of Physical Chemistry, Adam Mickiewicz University, Grunwaldzka 6, 60-780 Poznań, Poland

§Department of Chemical and Environmental Engineering, University of California, Riverside, California 92521-0425, United States

ABSTRACT: We use a classical density functional theory (DFT) to study the electric double layer formed by charged hard spheres near a planar charged surface. The DFT predictions are found to be in good agreement with recent computer simulation results. We study the capacitance of the charged hard-sphere system at a range of densities and surface charges and find that the capacitance exhibits a local minimum at low ionic densities and small electrode charge. Although this charging behavior is typical for an aqueous electrolyte solution, the local minimum gradually turns into a maximum as the density of the hard spheres increases. Charged hard spheres at high density provide a reasonable first approximation for ionic liquids. In agreement with experiment, the capacitance of this model ionic liquid double layer has a maximum at small electrode charge density.

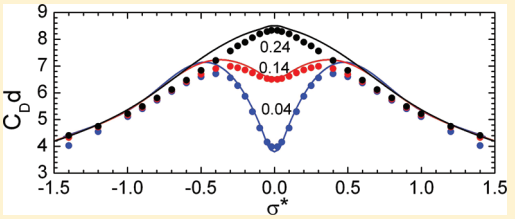

1. INTRODUCTION

An electric double layer is formed when a charged fluid is attracted to an electrode with the opposite charge. The Poisson−Boltzmann (PB) theory of Gouy, Chapman, and Stern (GCS)[1−3] is reasonable for a qualitative description of the ionic distributions in an aqueous electrolyte at low concentration in contact with an electrode that is not too highly charged. For practical applications, the GCS theory is convenient because it is analytic and easy for theoretical analysis. Although quantitatively lacking, it often can be made useful through adjustment of semiempirical parameters.

Ionic liquids are of practical interest, for example, in catalytic reactions, separation processes, and electronic devices. Basically, ionic liquids are room temperature molten salts. From our perspective, electric double layers formed by ionic liquids provide a valuable alternative system for theoretical study of inhomogeneous charged systems.[4] They do not involve the uncertainties and complexities of water, the usual solvent in conventional electrochemistry, and as such are comparatively straightforward model systems. Additionally, the density of the ions is comparatively high yet the direct electrostatic interactions are much stronger than those in water; they provide a new regime for theoretical study of ionic excluded volume effects and electrostatic correlations.

The GCS theory predicts that both the integral and differential capacitances show a minimum near the point of zero charge (PZC), i.e., the condition when the charge density of the electrode is zero. In addition, the GCS theory predicts that the differential capacitance becomes independent of the electrode charge when the surface charge density of the electrode or the ionic concentration is relatively high. The capacitance behavior predicted by the GCS theory is more or less true for electric double layers in aqueous systems. Although the experimental differential capacitance is not exactly independent of the electrode charge at high ionic concentration or high electrode charge density, this discrepancy between the GCS prediction and experiment is claimed to be due to the response of the water molecules near the electrode. High concentration double layers formed in aqueous systems cannot be examined experimentally because there is an upper limit to the solubility of ions in water.

In contrast, the capacitance (integral or differential) of the electric double layer of an ionic liquid often exhibits a maximum near the PZC.[4] Lamperski et al.[5] have made a Monte Carlo simulation of a simple ionic system that mimicks this behavior. They considered a system of charged hard spheres whose diameter is $d = 4$ Å and whose dimensionless temperature is $T^* = \varepsilon kTd/e^2 = 0.8$, where T is the temperature in K, k is the Boltzmann constant, and e is the magnitude of the elementary charge. Because there is no solvent in an ionic liquid, the dielectric constant, ε, is irrelevant here. It merely scales the temperature. All that matters is that we use the same value of T^* as Lamperski et al. They used $\varepsilon = 78.5$. Though the value of T^* is too large and/or the value of d is too small for a typical room-temperature ionic liquid, the system used by Lamperski et al.[5] seems to capture many features of a real ionic liquid. Because there are extensive simulation results available for this system, it is a convenient starting point for further theoretical studies. Lamperski et al.[5] found that at a low dimensionless density of all the ions, $\rho^* = Nd^3/V$, where N and V are the number of ionic spheres and the system volume, respectively, the capacitance has a local minimum at the PZC but as ρ^* increases,

Received: August 14, 2011
Revised: September 20, 2011
Published: October 04, 2011

this minimum becomes shallower, and at high enough ρ^* it becomes a maximum. Further, they applied the modified Poisson−Boltzmann (MPB) approximation[6] to this system and found good agreement with the simulation results at relatively low ionic density. Because the MPB equation does not converge for systems at high electrode charge, they did not test the performance of the MPB equation at such conditions. Following this, Lamperski and Henderson,[7] and subsequently, Outhwaite et al.[8] made simulations for the same system over a broader range of ionic densities and electrode charge densities, including conditions of high electrode charge densities. They found that at low ρ^*, the capacitance has a local minimum at the PZC and rises with an increasing magnitude of the dimensionless electrode charge, $\sigma^* = \sigma d^2/e$, where σ is the electrode charge density. The capacitance reaches a maximum and then falls with further increase of the magnitude of σ^*. On the other hand, at high ρ^*, the capacitance versus the surface charge exhibits a bell-shaped curve; i.e., it has a maximum at the PZC and falls with increasing or decreasing σ^*. Such behavior is beyond the GCS theory but is consistent with a plausible extrapolation of the MPB results.

Density functional theory (DFT)[9−16] has proven to be a useful theory for studying the structure and thermodynamic properties of inhomogeneous systems. Recently, DFT has been proposed as an alternative to the GCS theory for describing the electrochemical properties of electric double layers in ionic liquids.[17−19] In contrast to the GCS theory, DFT is able to account for the molecular excluded-volume effects and strong electrostatic correlations. In this paper, the DFT predictions are compared with the simulation results reported by Lamperski et al.[5,7,8] In particular, we examine the capacitance of charged hard-sphere systems over a wide range of densities and surface charges and potentials.

2. DENSITY FUNCTIONAL THEORY

The essential task in an application of DFT is to derive an analytical expression for intrinsic Helmholtz energy F or equivalently, grand potential Ω, as a functional of the underlying density profiles designated as $\rho_i(\mathbf{r})$. For ionic systems considered in this work, the grand potential and intrinsic Helmholtz energy are connected via the Legendre transformation:

$$\Omega = F + \int d\mathbf{r} \sum_i [\varphi_i(\mathbf{r}) - \mu_i] \tag{1}$$

where φ_i and μ_i stand for the one-body external potential and the chemical potential of ionic species i, respectively.

Near a planar electrode represented by a charged hard wall, the ionic density profiles vary only in the z direction, i.e., in the direction perpendicular to the electrode surface. At equilibrium, the grand potential is minimized with respect to the ionic density profiles, leading to the Euler−Lagrange equation:

$$\rho_i(z) = \rho_i \exp\{-\beta Z_i e\psi(z) + \beta\mu_i^{ex} - \delta\beta[F_{hs}^{ex} + F_{ec}^{ex}]/\delta\rho_i(z)\} \tag{2}$$

where $\rho_i = \rho_i(\infty)$ corresponds to the bulk ionic density of ionic species i, $\beta = 1/kT$, $\psi(z)$ stands for the local electric potential, Z_i represents the ionic valency (± 1 in our case), and F_{hs}^{ex} and F_{ec}^{ex} account for, respectively, the intrinsic Helmholtz energy due to the ionic size and that due to the electrostatic correlations. As detailed in our previous work,[14,15] F_{hs}^{ex} can be represented by a modified fundamental measure theory,[20−22] and F_{ec}^{ex} can be formulated in terms of a quadratic density expansion of the excess Helmholtz energy with respect to that of a uniform ionic system with the input of the direct correlation functions obtained from the mean-spherical approximation (MSA).[23,24]

Intuitively, eq 2 can be understood as a generalization of the Boltzmann equation for ionic distributions. Unlike the conventional Boltzmann equation for charged systems, however, eq 2 indicates that the structure of an inhomogeneous ionic system depends upon, in addition to the electrostatic potential, the ionic excluded volume and electrostatic correlation effects. Although both effects are ignored in the GCS theory, we expect that they play an important role in ionic liquids because, in comparison to a typical aqueous electrolyte solution, the ionic density is much higher and the electrostatic interaction is much stronger.

The Euler−Lagrange equation can be solved numerically with an iteration procedure. In the calculation of the charge distributions, we start with a prespecified surface electric potential, $\psi(0)$, and an initial guess for the density profiles of all ionic species, $\rho_i(z)$. The reduced mean electric potential is then calculated by integration of the Poisson equation:

$$\psi^*(z) \equiv \beta e\psi(z) = 4\pi l_B \sum_i \int_z^\infty dz' \, (z - z') Z_i \rho_i(z') \tag{3}$$

where $l_B = e^2/kT = d/T^*$ stands for the Bjerrum length. It is convenient in this work to write eq 3 in the following equivalent form:

$$\psi^*(z) = \psi^*(0) + 4\pi l_B \sum_i [\int_z^\infty dz' \, z Z_i \rho_i(z') + \int_0^z dz' \, z' Z_i \rho_i(z')] \tag{4}$$

From $\psi^*(z)$, we generate a new estimate for the density profiles from eq 2. The iteration process continues until that all density profiles have converged.

Once we have the equilibrium density profiles, the surface charge density is calculated from the condition of overall charge neutrality

$$\sigma = -e \sum_i \int_0^\infty dz' \, Z_i \rho_i(z') \tag{5}$$

The integral capacitance is given by

$$C_I = \sigma/\psi(0) \tag{6}$$

and the differential capacitance is defined as the derivative of the surface charge density with respect to the surface electric potential

$$C_D = \partial\sigma/\partial\psi(0) \tag{7}$$

Values for the capacitance can be obtained by using the reduced surface charge, σ^*, and surface potential, $\psi^*(0)$, in eqs 6 and 7. However, for direct comparison with the simulation results by Lamperski et al., these values have been multiplied by $\varepsilon d/T^*$, yielding Cd.

Although the DFT does not provide an explicit relation between σ and $\psi(0)$, eq 7 can be easily evaluated from a polynomial fitting of the electrode surface charge and potential relationship.

3. RESULTS

Values for the integral and differential capacitances are plotted in Figures 1 and 2, respectively, versus the dimensionless surface charge density of the electrode, $\sigma^* \equiv \sigma d^2/e$. The values of σ^* are

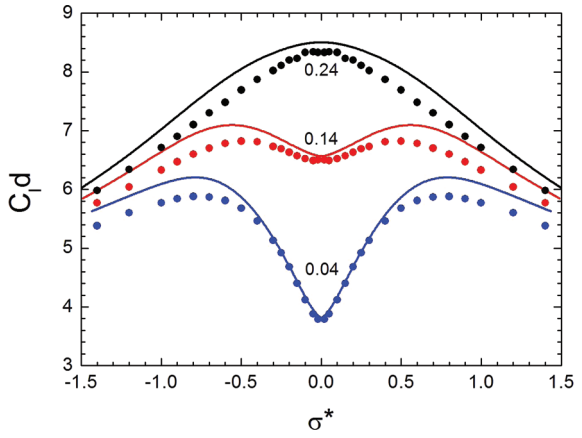

Figure 1. Integral capacitance, $C_I d$, for the dimensionless densities $\rho^* = 0.04$, 0.14, and 0.24 as a function of the dimensionless electrode charge density σ^*. The solid lines are DFT predictions, and the symbols are simulation results.[7,8]

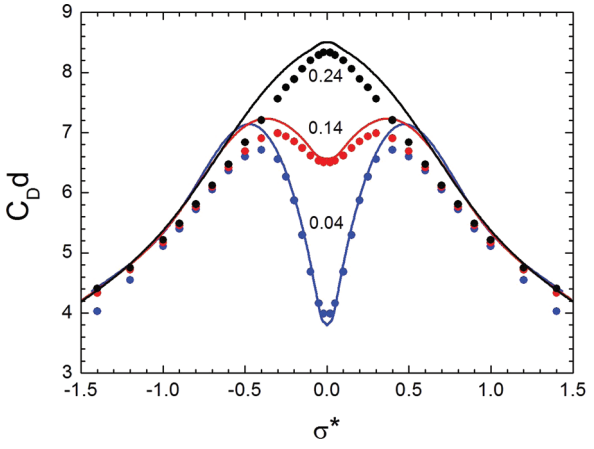

Figure 2. Differential capacitance, $C_D d$, for the dimensionless densities $\rho^* = 0.04$, 0.14, and 0.24 as a function of the dimensionless electrode charge density σ^*. The solid lines are DFT predictions and the symbols are simulation results.[7,8]

greater than that which is experimentially accessible, at least for low values of ρ^*. They were chosen in the simulation to expose the declining values of the capacitance at large σ^* and are considered here to demonstrate that DFT also exhibts this behavior. Here the DFT predictions (solid lines) are compared with the simulation results (symbols).[7,8] The agreement of the DFT capacitances with the simulation results is very good at all ionic densities. At the lowest ionic density, $\rho^* \equiv \rho d^3 = 0.04$, where $\rho = \rho_+ + \rho_-$ is the total ionic density, there is a local minimum at the PZC. This local minimum has almost disappeared at the intermediate density, $\rho^* = 0.14$. At the highest density, $\rho^* = 0.24$, both the integral and the differential capacitances exhibit a maximum at the PZC and the capacitance versus the surface charge density curve is bell shaped. The appearance of a bell-shaped capacitance curve is a feature of many ionic liquid double layers.[4,25] At high electrode charge densities, the differential capacitance is almost independent of the ionic density. The GCS theory makes this prediction but would have us believe that the capacitance curve is flat in this region.

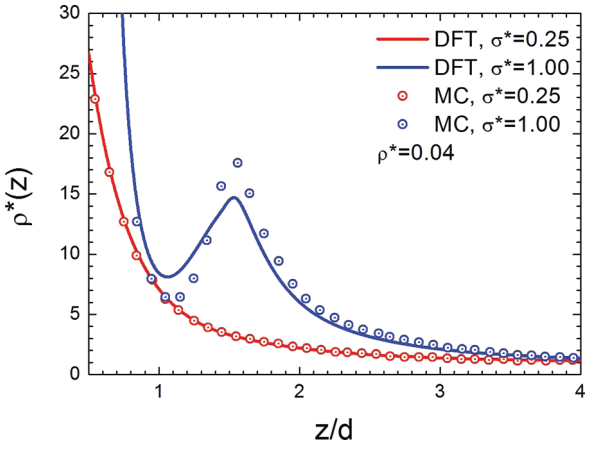

Figure 3. Counterion density profiles for $\rho^* = 0.04$ at two representative reduced surface charge densities, $\sigma^* = 0.25$ and 1.00.

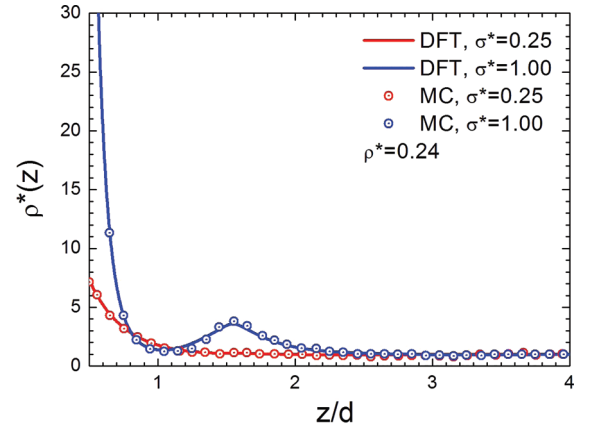

Figure 4. Counterion density profiles for $\rho^* = 0.24$ at two representative reduced surface charge densities, $\sigma^* = 0.25$ and 1.00.

The decline in the capacitance at high electrode charge is due to the fact that there is a limit to the number of ions that can be accommodated near the electrode. This saturation effect is clearly seen in Figures 3 and 4, where the counterion concentration profiles, $\rho^*(z)$, for $\rho^* = 0.04$ and $\rho^* = 0.24$ are plotted. As the electrode charge is increased, second- and higher-order peaks are formed near the surface. This ocillatory behavior was first seen in the simulations of Torrie and Valleau[26] and is a feature of all modern theories. The oscillatory density profiles are not just a result of the finite size of the ions, although this must surely play a role, but are also due to the electrostatic correlations among the ionic charges. As observed by Fedorov and Kornyshev,[25] the magnitude of the second and higher-order peaks at high electrode charge weakens (but does not vanish) as the electrode charge is increased. This is easily understood. In accord with the contact value condition of Henderson et al.,[27] the contact value of the density profile increases quadratically with the electrode charge. As the electrode charge increases, the contact value of the co-ion profile will become small. Thus, the contact value of the charge profile must increase quadratically with the electrode charge. On the other hand, the area of the charge profile, which must match the electrode charge, increases linearly with the electrode charge. As a result, the second and higher-order peaks must weaken in relation to the contact value. The

MPB equation predicts oscillatory profiles but cannot shed any light on the decrease of the capacitance at large electrode charge because it fails to give convergent solutions under this conditions. Both effects are missing in the GCS theory, which predicts monotonically decreasing profiles. The agreement of the DFT profiles with those obtained from the simulations is again very good.

4. SUMMARY

We have compared the results of the DFT predictions for model electric double layers with simulation results and investigated the capacitance of a high density ionic system that captures some of the key features of the electric double layers of ionic liquids. The agreement of the DFT with simulation is very good. However, the DFT considered here is not perfect. One interesting feature that is seen in recent simulations[28,29] is that at very low values of T^* and ρ^*, a depletion layer of ions forms near the electrode. Such depletion is not seen in the MSA or the version of DFT considered here, probably because the MSA direct correlation function is employed. Neither the MSA or the DFT considered here predicts values of the average profile at contact that are less than the bulk density. It is always good to be able to look forward to the opportunity for theoretical improvement. However, the problem that we just mentioned is not relevant to ionic liquid double layers because the value of the contact value of the ionic density profile is always large. In any case, even in its present state of development, DFT is able to shed light on ionic liquids and such phenomena as dispersion forces, molecular structure, and polarization.

AUTHOR INFORMATION

Corresponding Author
*E-mail: doug@chem.byu.edu.

ACKNOWLEDGMENT

This work is in part supported by the National Science Foundation (NSF-CBET-0852353) and by the U.S. Department of Energy (DE-FG02-06ER46296). The financial support from Adam Mickiewicz University, Faculty of Chemistry, is appreciated.

REFERENCES

(1) Gouy, M. *J. Phys. (Paris)* **1910**, *9*, 457–468.
(2) Chapman, D. L. *Philos. Mag.* **1913**, *25*, 475–481.
(3) Stern, O. *Z. Elektrochem.* **1924**, *30*, 508–516.
(4) Kornyshev, A. A. *J. Phys. Chem. B* **2007**, *111*, 5545–5557.
(5) Lamperski, S.; Outhwaite, C. W.; Bhuiyan, L. B. *J. Phys. Chem. B* **2009**, *113*, 8925–8929.
(6) Outhwaite, C. W.; Bhuyian, L. B. *J. Chem. Soc., Faraday Trans. 2* **1983**, *79*, 707–718.
(7) Lamperski, S.; Henderson, D. *Mol. Simul.* **2011**, *37*, 264–268.
(8) Outhwaite, C. W.; Lamperski, S.; Bhuiyan, L. B. *Mol. Phys.* **2011**, *109*, 21–26.
(9) Evans, R., Density functionals in the theory of nonuniform fluids. In *Fundamentals of Inhomogeneous Fluids*; Henderson, D., Ed.; Marcel Dekker: New York, 1992; pp 85−175.
(10) Tang, Z.; Mier y Teran, L.; Davis, H. T.; Scriven, L. E.; White, H. S. *Mol. Phys.* **1990**, *71*, 369–392.
(11) Mier y Teran, L.; Tang, Z.; Davis, H. T.; Scriven, L. E.; White, H. S. *Mol. Phys.* **1991**, *72*, 817–830.
(12) Groot, R. D. *Mol. Phys.* **1987**, *60*, 45–63.
(13) Patra, C. N.; Ghosh, S. K. *J. Chem. Phys.* **1994**, *100*, 5219–5229.
(14) Wu, J. Z. *AIChE J.* **2006**, *52*, 1169–1193.
(15) Wu, J. Z.; Li, Z. D. *Annu. Rev. Phys. Chem.* **2007**, *58*, 85–112.
(16) Gillespie, D.; Valiskó, M.; Boda, D. *J. Phys.-Condens. Mater.* **2005**, *17*, 6609–6626.
(17) Forsman, J.; Woodward, C. E.; Trulsson, M. *J. Phys. Chem. B* **2011**, *115*, 4606–4612.
(18) Jiang, D. E.; Meng, D.; Wu, J. Z. *Chem. Phys. Lett.* **2011**, *504*, 153–158.
(19) Wu, J. Z.; Jiang, T.; Jiang, D. E.; Jin, Z. H.; Henderson, D. *Soft Matter* **2011**, DOI: 10.1039/c1sm06089a.
(20) Rosenfeld, Y. *Phys. Rev. Lett.* **1989**, *63*, 980–983.
(21) Yu, Y. X.; Wu, J. Z. *J. Chem. Phys.* **2002**, *117*, 10156–10164.
(22) Roth, R.; Evans, R.; Lang, A.; Kahl, G. *J Phys.-Condens. Mater.* **2002**, *14*, 12063–12078.
(23) Yu, Y. X.; Wu, J. Z.; Gao, G. H. *J. Chem. Phys.* **2004**, *120*, 7223–7233.
(24) Blum, L. *Mol. Phys.* **1975**, *30*, 1529–1535.
(25) Fedorov, M. V.; Kornyshev, A. A. *J. Phys. Chem. B* **2008**, *112*, 11868–11872.
(26) Torrie, G. M.; Valleau, J.-P. *J. Chem. Phys.* **1980**, *73*, 5807–5816.
(27) Henderson, D.; L. Blum, L.; Lebowitz, J. L. *J. Electroanal. Chem.* **1979**, *102*, 315–319.
(28) Boda, D.; Henderson, D.; Chan, K. Y.; Wasan, D. T. *Chem. Phys. Lett.* **1999**, *308*, 473–478.
(29) Di Caprio, D.; Valiskó, M.; Holovko, M.; Boda, D. *Mol. Phys.* **2006**, *104*, 3777–3786.